Available online at www.sciencedirect.com
SCIENCE DIRECT®
Bioorganic & Medicinal Chemistry 12 (2004) 4233–4244
Bioorganic & Medicinal Chemistry

DNG cytidine: synthesis and binding properties of octameric guanidinium-linked deoxycytidine oligomer

Istvan E. Szabo and Thomas C. Bruice*

Department of Chemistry and Biochemistry, University of California, UCSB, Santa Barbara, CA 93106, USA

Received 27 February 2004; revised 7 May 2004; accepted 7 May 2004
Available online 19 June 2004

Abstract—The synthesis of guanidinium-linked cytidyl oligomer (DNG-C_8), a cationic DNA analog, and the corresponding cytidine monomers is described. The DNG monomer synthesis was streamlined to produce a shorter route to the final monomer than previously reported for thymidine and subsequent solid-phase synthesis produced an octameric cytidyl DNG strand. Because octameric deoxyguanosine would be used as the complementary strand in our studies, it was necessary to investigate guanosine self-association. Singular value decomposition was used to mathematically deconvolve the spectral data and confirm the presence of transitions due to DNA-G_8 self-association. Job plots show the binding stoichiometry of DNG-C_8 with DNA-G_8 to be 1:1. Thermal denaturation studies of the DNG-C_8·DNA-G_8 duplex established a $T_m \geqslant 90\,^{\circ}C$ and a $\Delta G^{\circ} = -13.3\,kcal\,mol^{-1}$, indicating the DNG-$C_8$·DNA-$G_8$ duplex is over 1000 times more stable than that of DNA-C_8·DNA-G_8.

1. Introduction

Oligonucleotide analogs capable of recognizing and binding complementary RNA and DNA with the intended purpose of arresting cellular processes at the translational and transcriptional level are known as antisense and antigene agents,[1,2] respectively. Key goals in designing antisense/antigene agents are the following: high specificity to and affinity for the target sequence, stability in the presence of cellular nucleases and membrane permeability. In the specific case of RNA targeted antisense therapy, RNase H activation[3] is a desirable feature. Since antisense agents were first introduced, a diverse range of analogs have been developed. Substitution of the phosphodiester oxygens while preserving the phosphate core results in the formation of such analogs as phosphorothioates, phosphoroamidates, and methylphosphonates,[4] while total replacement of the furanose–phosphate moiety with peptide linkages results in peptide nucleic acids (PNA),[5] PHONA,[6] and PNAA.[7] These neutral linkages eliminate the mutual repulsion seen in the anionic backbones of duplex DNA and are resistant to nucleases. Other variations on the internucleoside linker theme include morpholino,[8] methylenemethylimino,[9] carbamates,[10] acetals,[11] heterocycles,[12] and locked nucleic acids.[13]

In recent years, approaches involving the incorporation of positive charges in antisense oligomers have been developed. Positive charges can be added to the bases[14] or the sugar rings to give zwitterionic DNA.[15] The phosphate backbone and phosphoramidate linkages can be alkylated with alkylamines to produce positively charged phosphate triester linkages[16,17] and cationic phosphoramidate linkages.[18] A promising approach designed by this laboratory is the replacement of internucleoside phosphate linkage with an achiral, positively charged guanidinium group[19] (Fig. 1). This species, designated as DNG, for deoxy-nucleic-guanidine, exhibits high affinity and specificity for DNA as well as resistance to nucleases.[20] Thymidyl DNG oligomers have been demonstrated to have a high affinity for, and bind in a 2:1 stoichiometry with, complementary adenyl DNA oligomers,[21] while DNG-A oligomers form 1:2 complexes with thymidyl DNA oligomers.[22] A guanidinium linked RNA analog is currently in development.[23,24]

The guanidinium chemistry described here proceeds in the $3' \rightarrow 5'$ direction and is compatible to standard solid-phase DNA synthesis, making it possible for the design of DNG/DNA chimera. To this date, DNG oligonucleotides have been synthesized with only adenyl and

Keywords: Oligomer; Monomer; DNA; Antisense/antigene.
* Corresponding author. Tel.: +1-80-5893-2234; fax: +1-80-5893-2229; e-mail: tcbruice@chem.ucsb.edu

0968-0896/$ - see front matter © 2004 Elsevier Ltd. All rights reserved.
doi:10.1016/j.bmc.2004.05.010

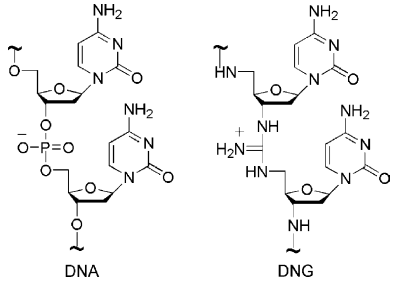

Figure 1. Structure of phosphodiester and guanidinium linkage.

thymidyl moieties. We present in this report, for the first time, the total synthesis of the cytidine DNG monomer and solid-phase synthesis of octameric cytidyl DNG, as well as a preliminary investigation into DNG-C_8 binding properties with natural DNA-G_8.

2. Results and discussion

Since their inception, the synthesis of DNG oligomers has evolved dramatically. Initially, the synthesis of the oligomers occurred in the $5' \rightarrow 3'$ direction, resulting in a backbone comprised of intermediate thiourea linkages which were subsequently oxidized and amidated to provide the desired guanidinium linkages.[25] Ultimately the direction of oligomer synthesis was reversed to run $3' \rightarrow 5'$ and protected guanido groups were formed during monomer coupling reactions. During oligomer cleavage from the solid support, the guanido groups were deprotected to provide the guanidinium linkages.[22] Synthesis in the $3' \rightarrow 5'$ direction has the added advantage of being compatible with standard DNA technologies, making DNA/DNG chimera feasible.

The coupling reaction (Scheme 1) proceeded with the abstraction of the sulfur atom from an Fmoc-protected thiourea using mercury(II) and transformed the thiourea into an activated carbodiimide, which reacted readily with a free amino group to give the protected guanido linkage. The use of long-chain-alkylamine controlled pore glass is now preferred to polystyrene resin as a solid support because the oligomer can be removed easily from the glass using methanolic ammonia, a step which also removes all base labile protecting groups from the oligomer. The controlled pore glass (CPG) was first loaded with a 'primer' monomer using a base labile succinyl-ester linkage following a standard procedure.[26]

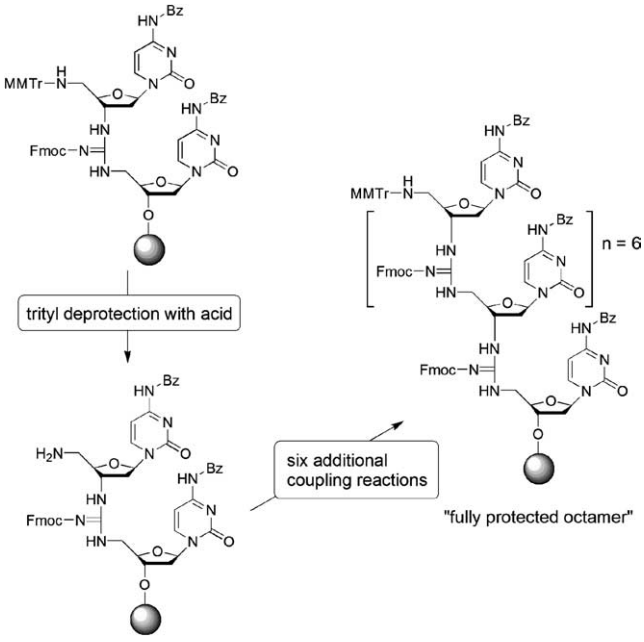

Scheme 2. 5′-Trityl is removed to expose amine for the next coupling reaction.

This loading monomer is a N^4-benzoyl-5′-MMTr-NH-3′-O-succinate derivative of **8**, which was prepared from the 2′-deoxycytidine starting material (Scheme 4). Formation of Hg_2S from HgS often results during the course of the coupling reaction, precipitating out and turning the solution and glass support a dark gray color. This Hg_2S precipitate was removed by the addition of 20% thiophenol in DMF.

Acetic anhydride was used to acylate any unreacted amines, thereby capping incompletely coupled oligomers. The 5′-trityl group of the terminal monomer was removed with dichloroacetic acid in order to regenerate the 5′-amino moiety necessary for the coupling reaction to follow (Scheme 2). The process was repeated until the oligomer of desired length was achieved. The 5′-trityl protecting group was allowed to remain after the last coupling reaction in order to facilitate purification.

Cleavage and partial deprotection of the oligomer was performed in one step, which consists of soaking the CPG in methanolic ammonia overnight at 60 °C (Scheme 3). The supernatant was concentrated to a white powder and re-dissolved in 10% acetonitrile in

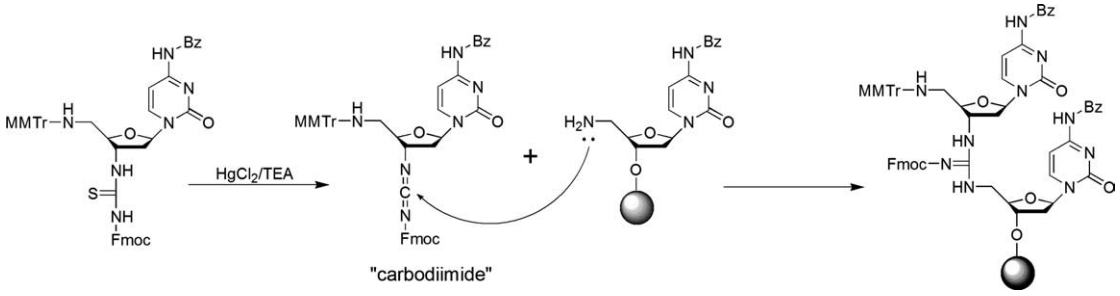

Scheme 1. First step in monomer coupling is the formation of the carbodiimide and subsequent addition to form the protected guanido group.

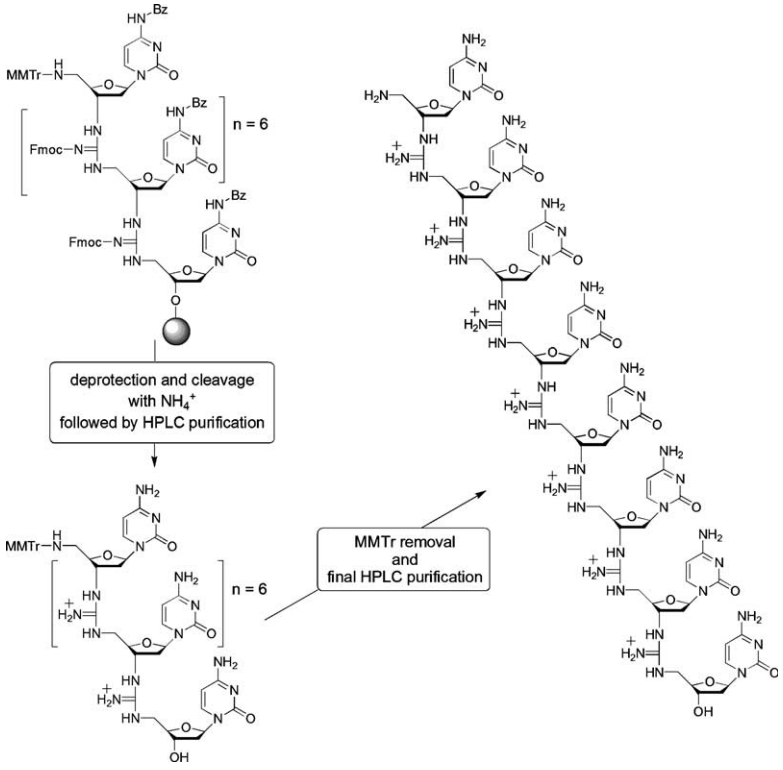

Scheme 3. Cleavage from CPG, deprotection of guanido groups and nucleobases occurs in one step using methanolic ammonia at 60 °C.

triethylammonium acetate buffer for reverse-phase (RP) HPLC purification. Because acetic anhydride was used to cap all uncoupled amines after each coupling reaction and the 5′-MMTr protecting group was not removed after addition of the last monomer, purification of the final oligomer was straightforward.

Using a balance of aqueous buffer and organic solvent as eluents, 'trityl-on' purification easily separated incompletely coupled oligomers from the trityl-protected final oligomer. Following purification, the trityl group was removed with 2% dichloroacetic acid in methylene chloride and the oligomer was again purified by RP-HPLC.

The synthesis of the final cytidine coupling monomer (Scheme 4) began with benzoylating commercially available 2′-deoxycytidine, using an established transient protection method,[26] in order to protect the *exo*-cyclic amine on the nucleobase. The resultant N^4-benzoyl-2′-deoxycytidine **1** was treated with excess methanesulfonyl chloride to provide 3′,5′-dimesyl deoxycytidine **2**. Refluxing a DMF solution of **2** with potassium phthalimide displaced the 3′-mesyl and formed a 2,3′-anhydro species **3**, preserving the 5′-mesyl moiety.[27] Treatment of **3** with LiN_3 in DMF displaced the 5′-mesyl group and broke the 2,3′-anhydro bond resulting in 3′,5′-diazido-N^4-benzoyl cytidine **4**. Catalytic hydrogenation of the azides to amines using activated carbon and hydrogen

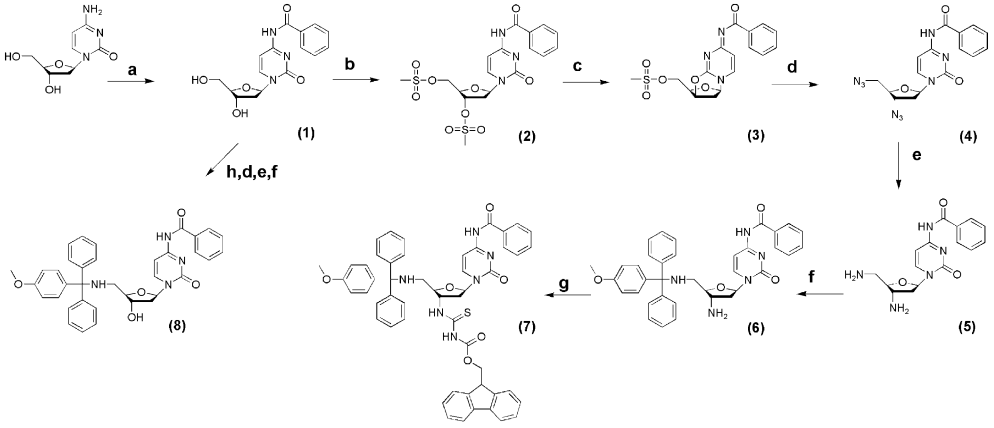

Scheme 4. Reagents and conditions: (a) BzCl/pyridine; (b) MsCl/pyridine; (c) KPhTh/DMF; (d) LiN_3/DMF; (e) $H_{2(g)}$/Pd–C/EtOH; (f) MMTrCl/pyridine; (g) Fmoc-NCS/pyridine; (h) TsCl/pyridine; (d) LiN_3/DMF; (e) $H_{2(g)}$/Pd–C/EtOH; (f) MMTrCl/pyridine.

gas gave 3′,5′-diamino-N^4-benzoyl cytidine **5**, which was reacted with 0.9 equiv of MMTrCl in pyridine at −70 °C to yield the 5′-MMTr-NH derivative **6**. Although a small amount of ditritylated product formed, it was easily separated by silica gel chromatography. Lastly, **6** was reacted with 9-fluorenylmethoxy-carbonylisothiocyanate[23,28] in pyridine to give N^4-benzoyl-3′-Fmoc-NCS-5′-MMTr-NH-2′deoxycytidine **7**.

2.1. Physical properties

It is well known that DNA rich with deoxyguanosine can form complex noncovalent secondary structures with itself, namely G-quadruplexes and tetraplexes.[29,30] Given that octameric deoxyguanosine (DNA-G_8) would be needed to complement our DNG-C_8, it was necessary to determine whether octameric guanosine self-association would present a problem. Although deoxycytosine can also self-associate to form double helices[31] and *i*-motifs,[32] this generally requires a low pH to protonate the cytosine N^3 ($pK_a = 4.17$).[33] DNA-C_8, in our working buffer ([KCl] = 100 mM; [$KHPO_4$] = 10 mM; pH 7), was heated to 90 °C and showed no increase in absorbance with respect to temperature. Additionally, the overall positive charge of DNG-C_8 strongly disfavors self-association.[34] Binding stoichiometry was determined by performing Job plots[35] on DNA and DNG hexomeric oligomers (see Methods). For both the DNA-C_6·DNA-G_6 and DNG-C_6·DNA-G_6 mixtures, the binding was determined to be 1:1 (Fig. 2). This binding stoichiometry suggests the formation of a duplex DNG·DNA strand with Watson–Crick base pairing. Although the possibility of other base pairing arrangements exist,[36] they are unlikely to be formed in a an aqueous solution buffered to pH 7. Furthermore, previously published computational[37] and circular dichroism[21] studies provide evidence that the base pairing is indeed Watson–Crick and the bound DNG·DNA strands are helical in structure.

In order to confirm that the observed transitions were indeed from deoxyguanosine and deoxycytidine base-pairing, rather than deoxyguanosine self-association, we deconvolved the spectra to determine the number of species undergoing transition. If a heated solution of DNA-C_8·DNA-G_8 also contained DNA-G_8 self-associated structures, the transitions for all of the species would be included the spectrum. We employed singular value decomposition (SVD), a linear algebra based computational[38] method, to analyze the melting data. SVD factors the input matrix, A (representing spectral absorption values), into three matrices, U, V^T and S, where superscript T indicates V is transposed and S is a diagonal matrix. Much of the insight into applying SVD to deconvolve spectra has been provided by work of Henry and Hofrichter,[39] Hendler and Shrager,[40] and Haq et al.[41]

The data set is created by scanning the sample from 300 to 220 nm at every degree as the sample is heated from 5 to 90 °C at a rate of 0.5 °C/min. The result can be visualized as a 3-D surface (Fig. 3). This absorbance data is arranged into a matrix, A, containing absorbance values whose columns represent temperature and rows represent wavelengths. SVD expresses matrix A as the product of three matrices, USV^T. The diagonal matrix S contains the square roots, or singular values, of the eigenvalues for the vectors specified in U and V. The singular values of S are a measure of weight, in terms of value, for those columns in U and V, and indicate the number of significant spectral species.

A plot of the (diagonal entry number in matrix S) versus ($10 \times \log$ of that value) yields a curve which begins to deviate sharply for entry numbers 1–5 (Fig. 4) for DNA-G_8 and DNA-C_8·DNA-G_8, suggesting that there are at most five statistically significant singular values. Autocorrelation calculations were performed in order to measure the 'signal-to-noise' ratio in the column vectors of V and determine which columns contained valid information and, therefore, the number of significant singular values. Eq. 1 was used, along with the established criterion of $C(V_i) \geqslant 0.8$ for vectors with a strong 'signal',[39] to confirm that there were at most five sig-

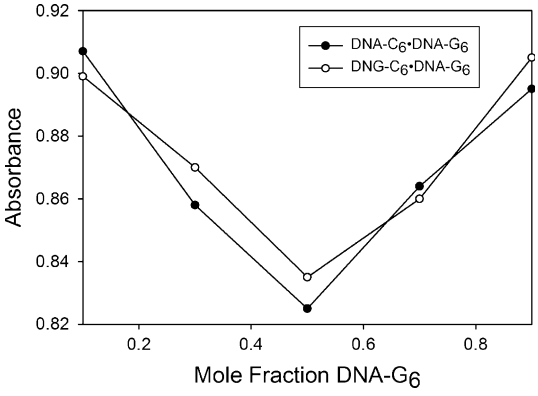

Figure 2. Job plot illustrating 1:1 binding of DNA-C_6, and DNG-C_6, to DNA-G_6. Total oligomer concentration was 12 μM and buffer contained 100 mM [KCl], 10 mM [$KHPO_4$], adjusted to pH 7.

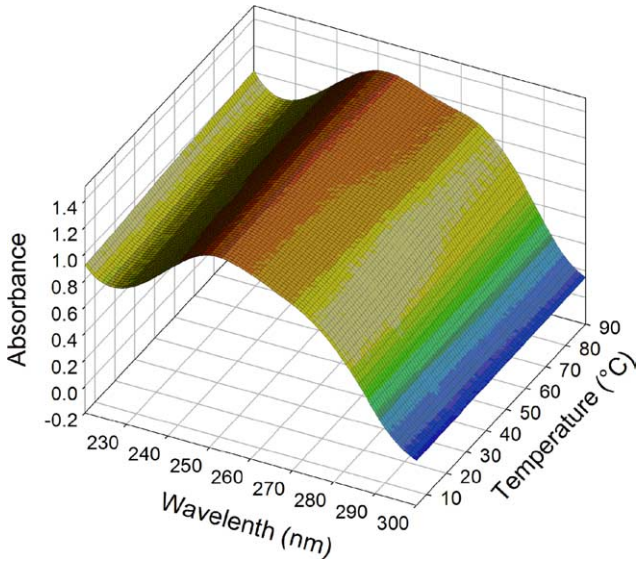

Figure 3. 3-D mesh plot of DNA-C_8·DNA-G_8 melting. Wavelength scans (300–220 nm) are taken every degree as sample is heated from 5 to 90 °C at a rate of 0.5 °C/min. ([DNA] = 15 μM; [KCl] = 100 mM; [$KHPO_4$] = 10 mM; pH 7).

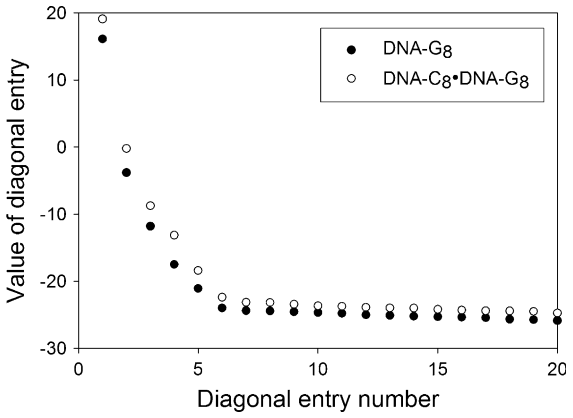

Figure 4. Plot of $10 \times \log$ (singular value) versus position in matrix S reveals that 1–5 appear significant for the samples DNA-G_8 and DNA-C_8·DNA-G_8.

nificant singular values for both DNA-G_8 and DNA-C_8·DNA-G_8 (data not shown).

$$C(V_i) = \sum_{j=1}^{n-1} V_{j,i} V_{j+1,i} \qquad (1)$$

$V_{j,i}$ is the jth element in the ith column of matrix V.

A difference spectrum involves creating a new D matrix, from matrices V and U using a minimum number of S values, then subtracting D from the original matrix A and plotting the difference. Selecting the correct number of S values will produce a difference plot containing only noise. For the sample containing only DNA-G_8, the difference spectra computed with three singular values gave rise to randomness in the plot (Fig. 5). Note that four singular values did not increase this randomness. This indicates that for DNA-G_8, three singular values are statistically significant. Difference spectra for DNA-C_8·DNA-G_8 indicates there are four significant singular values, one more than for DNA-G_8 (Fig. 6).

Although the DNA-G_8 sample contained multiple transitions, we cannot say exactly what structures they arise from. However, we can say that these transitions also occur in the DNA-C_8·DNA-G_8 sample, indicating that deoxyguanosine self-association occurs even in presence of deoxycytosine. SVD clearly indicates that the sample containing DNA-C_8·DNA-G_8 has one more transition than the sample containing only DNA-G_8, due to the interaction of deoxyguanosine and deoxycytidine residues.

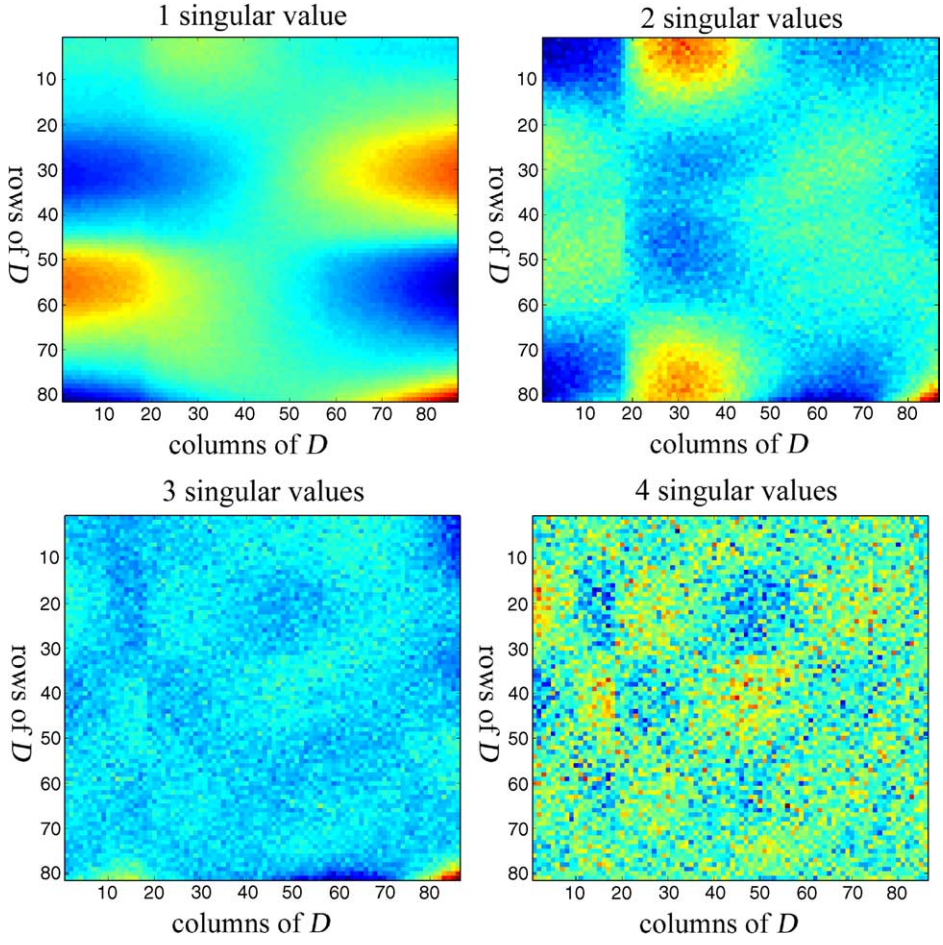

Figure 5. Plots of difference matrix, D, for the first four singular values of the diagonal matrix S for DNA-G_8. The plot generated using three singular values (lower left) shows a complete subtraction of the spectrum, leaving only noise.

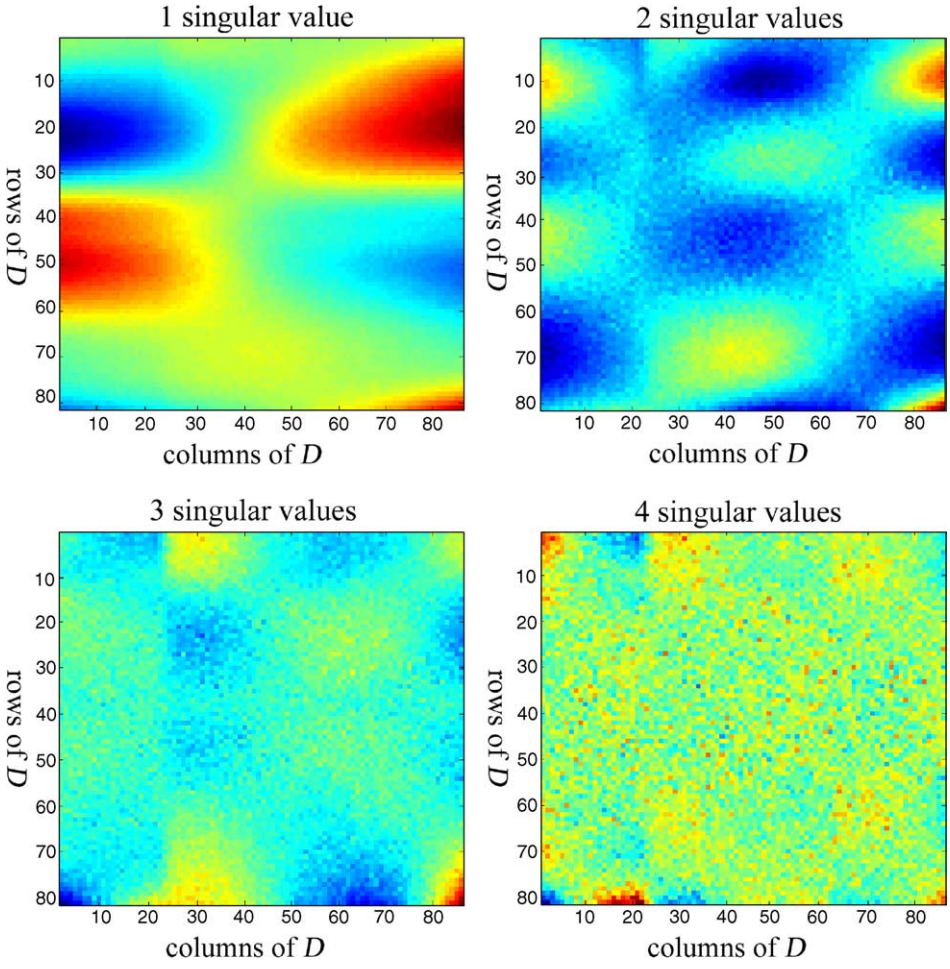

Figure 6. Plots of difference matrix, D, for the first four singular values of the diagonal matrix S for DNA-C_8·DNA-G_8. The plot generated using four singular values (lower right) shows a complete subtraction of the spectrum, leaving only noise.

2.2. Thermodynamic calculations

While repetitive scanning over multiple wavelengths is used for SVD, thermal denaturation studies monitor the absorbance at a constant wavelength. Although deoxyguanosine has a λ_{max} at 252 nm, it shows the largest temperature-correlated absorbance between 270 and 275 nm. Given that deoxycytidine has a λ_{max} at 272 nm, we chose that as the wavelength to observe.

At 272 nm, DNA-G_8 has a clear transition at ~50 °C, due to the thermal disassociation of a secondary structure (Fig. 7).

The melting curves for DNA-C_8·DNA-G_8 and DNG-C_8·DNA-G_8, at 272 nm, indicate that two very different transitions are occurring (Fig. 8). DNA-C_8·DNA-G_8 shows a typical melting curve with a T_m at 38 °C, while DNG-C_8·DNA-G_8 shows a long upward inflection, suggestive of the lower half of a sigmoid curve. The published melting temperatures for DNG-T_8·DNA-A_8 and DNG-TA_5·DNA-T_8 are 63 and 79 °C, respectively, while the T_m of their respective DNA·DNA counterparts is below 10 °C.[21,22] Assuming a similar increase in T_m, and given that the T_m of DNA-C_8·DNA-G_8 was experimentally determined to be 38 °C, the melting temperature of our DNG-C_8 with complementary DNA-G_8 is expected to be above 90 °C.

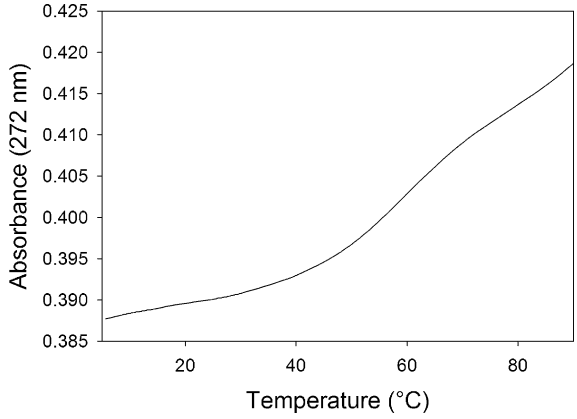

Figure 7. The melting curve of octameric deoxyguanosine at 272 nm; heated from 5 to 90 °C ([DNA] = 3 μM; [KCl] = 100 mM; [$KHPO_4$] = 10 mM; pH 7).

In a binding study of DNG-T with DNA-A, we found that an increase in ionic strength (μ) results in a decrease

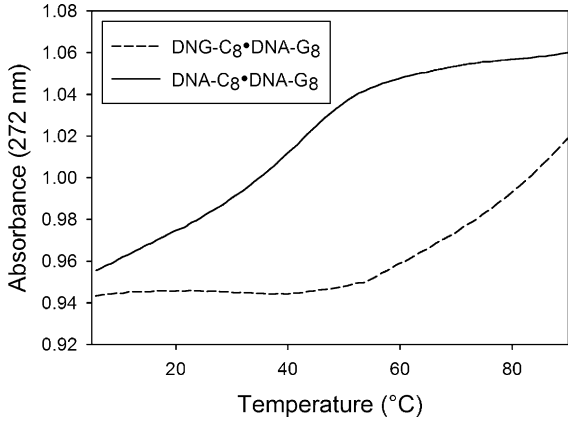

Figure 8. The melting curves of DNA-C_8·DNA-G_8 and DNA-C_8·DNG-G_8 heated from 5 to 90 °C ([DNA:DNA] = 7.5 μM; [DNA:DNG] = 7.5 μM; [KCl] = 100 mM; [$KHPO_4$] = 10 mM; pH 7).

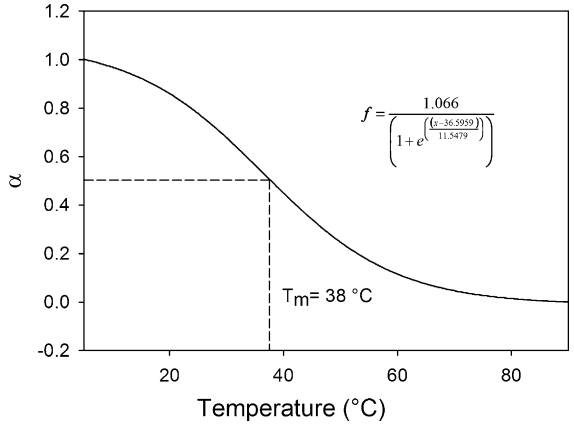

Figure 9. Plot of 'α versus temperature' for DNA-C_8·DNA-G_8.

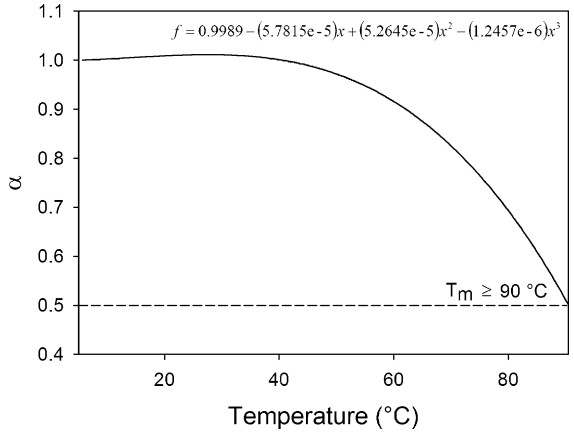

Figure 10. Plot of 'α versus temperature' for DNG-C_8·DNA-G_8.

in the DNG·DNA melting temperature. This μ affect is opposite to that seen with DNA·DNA interactions and is attributed to salt ions disrupting the favored electrostatic attraction between the negative phosphates and the positive guanidiniums. Increasing monovalent cation concentration, specifically sodium or potassium, stabilizes the formation of guanosine quartets, which are unable to hydrogen-bond with cytosine residues.[42,43] Thus, when μ of solutions containing either DNA-C_8·DNA-G_8 or DNG-C_8·DNA-G_8 oligomers was increased, from 0.13 to 0.33 and 0.53, we observed no hyperchromic shift.

Following the work of Marky and Breslauer,[44] we calculated the thermodynamic data for the melting transitions of DNA-C_8·DNA-G_8 and DNG-C_8·DNA-G_8. The first step is to convert the experimental 'absorbance versus temperature' curve into an 'α versus temperature' profile (Figs. 9 and 10). Defining α as being equal to the fraction of single strands in the duplex state, we can state that if x is the height between the absorbance curve and upper baseline, or last absorbance value, and $(x + y)$ is the height between the upper and lower baselines, or first and last absorbance values, then $\alpha = x/(x + y)$.

The goal is to use this new 'α versus temperature' plot to find the value for the term $(\partial\alpha/\partial T)_{T=T_m}$ in the van't Hoff equation (Eq. 2), where the $n = 2$ (strand molecularity), $T_m = 311.15\,K$, and $R = 1.9872\,cal\,mol^{-1}\,K^{-1}$. Because $(\partial\alpha/\partial T)_{T=T_m}$ is the slope of the curve for 'α versus temperature' at $\alpha = 1/2$ and $T = T_m$, computational methods can be used to get an equation $f(x)$, which fits the α versus temperature' curve, and calculate its first derivative $f'(x)$, evaluating it at T_m. At the melting temperature T_m where $\alpha = 1/2$, the equilibrium constant for non-self-complementary sequences is given by (Eq. 3), where C_T is the total strand concentration (15 μM) and $n = 2$. $\ln K(T)$ is given by (Eq. 4), where $T = 298.15\,K$, and ΔG° is given by (Eq. 5).

$$\Delta H_{VH} = (2 + 2n)RT_m^2\left(\frac{\partial\alpha}{\partial T}\right)_{T=T_m} \tag{2}$$

$$K_{T_m} = \frac{1}{(C_T/2n)^{n-1}} \tag{3}$$

$$\ln K(T) = \ln K(T_m) - \frac{\Delta H_{VH}}{R}\left(\frac{1}{T} - \frac{1}{T_m}\right) \tag{4}$$

$$\Delta G^\circ = -RT\ln K(T) \tag{5}$$

Table 1 summarizes the thermodynamic results and parameters used for DNA-C_8·DNA-G_8 and DNG-C_8·DNA-G_8, clearly demonstrating the tighter binding of DNG to its DNA template. Because DNG-C_8·DNA-G_8 appears to have a T_m at or above the temperature limit of the experiment, we used a conservative estimate of $T_m = 90\,°C$ for our calculations and defined $\alpha = 1/2$ at that temperature. The $\Delta\Delta G^\circ$ of $-4.8\,kcal\,mol^{-1}$ translates into over three orders (3.4) of magnitude increase in binding. This means that DNG-C_8 binds DNA-G_8 over 1000 times more tightly than DNA-C_8. This increase is attributed to the powerful attraction between the positively charged DNG guanidinium groups and negatively charged phosphates of DNA.

The strength and fidelity of the G·C base pair, due to three hydrogen bonds, in combination with the electrostatic attraction of DNG for DNA suggests that

Table 1. Thermodynamic data and parameters for DNA-C_8·DNA-G_8 and DNG-C_8·DNA-G_8

	DNA-C_8·DNA-G_8	DNG-C_8·DNA-G_8
Regression equation	$f = \frac{y_0 + a}{\left(1 + e^{\left(\frac{-(x-x_0)}{b}\right)}\right)}$	$f = y_0 + ax + bx^2 + cx^3$
Parameters	$a = 1.0762$	$y_0 = 0.9989$
	$b = -11.5479$	$a = -5.7815 \times 10^{-5}$
	$x_0 = 36.5959$	$b = 5.2645 \times 10^{-5}$
	$y_0 = -0.0102$	$c = -1.2457 \times 10^{-6}$
T_m	38 °C	90 °C
$\partial\alpha/\partial T$	−0.0230	−0.0209
ΔH_{VH}	−26.5 kcal mol^{-1}	−32.9 kcal mol^{-1}
$\ln K(T)$	14.3660	22.4218
ΔG°	−8.5 kcal mol^{-1}	−13.3 kcal mol^{-1}

strategically placed guanidinium-linked cytidines in a DNA/DNG chimera may yield a powerful antisense combination.

3. Experimental

3.1. Materials

All anhydrous solvents, triethylamine, methane sulfonyl chloride, monomethoxy trityl chloride, 9-fluorenylmethylchloroformate, mercury(II) chloride, and potassium isothiocyanate were purchased through Aldrich and used without further purification. HPLC grade triethylammonium acetate buffer was purchased from Fluka, HPLC grade acetonitrile was purchased from Fisher, long-chain-alkylamine controlled pore glass was purchased from Sigma, ammonia gas was purchased from Matheson, and the 2′-deoxycytidine monohydrate starting material was purchased from Acros.

3.2. General

Hydrogenations were carried out with a Parr hydrogenator equipped with a 500 mL hydrogenation vessel. TLC was carried out on silica gel (Kieselger 60 F_{254}) glass-backed commercial plates and visualized by UV light. ^{1}H and ^{13}C NMR spectra were obtained on a Varian Unity 500 MHz. Analytical reverse phase HPLC was performed on a Hewlett–Packard 1050 system equipped with a quaternary solvent delivery system and UV detector set at 260 nm and a 10 × 250 mm Macrosphere C8 reverse-phase column purchased from Altech. UV spectra, thermal studies and Job plots were obtained on a Cary 100 Bio UV/vis spectrophotometer equipped with a temperature programmable cell block and a PC interface running Cary WinUV software from Varian, Inc.

3.3. Thermal denaturation experiments

DNA-C_8·DNA-G_8 and DNG-C_8·DNA-G_8 samples were dissolved in a 1:1 stoichiometry, with a total oligomer concentration of 15 μM, in buffer containing 100 mM [KCl], 10 mM [$KHPO_4$], adjusted to pH 7. Samples were covered with a layer of mineral oil and heated to 90 °C, allowed to cool to room temperature, then stored in a 4 °C refrigerator overnight. The samples were placed in the spectrophotometer's Peltier heating block, the temperature was ramped from 5 to 90 °C at a rate of 0.5 °C min^{-1} under an atmosphere of nitrogen gas, and data was collected at 1 °C intervals.

3.4. Job plots

Five 1 mL samples were prepared identically to the thermal denaturation procedure, using the same buffer and annealing conditions, each with a different mole fraction of deoxycytidine and deoxyguanosine oligomers. The mole fraction of each strand was varied from 0.1 to 0.9, in 0.2 increments, while the total strand concentration was kept at 12 μM. The absorption of each sample was recorded at room temperature and the results were plotted against mole fraction of oligomer in order to determine the binding stoichiometry.

3.5. Solid-phase synthesis of octameric cytidyl DNG

3.5.1. Loading. Commercially available long-chain-alkylamine controlled pore glass (CPG), with 500 Å pore size and 80–120 mesh size, was used as the solid support and the N^4-benzoyl-3′-hydroxy-5′-NH-MMTr-2′,5′-deoxycytidine monomer **8** was loaded onto the support as the 3′-succinyl ester using standard methods. UV analysis of the trityl cation released upon treatment with 2% dichloroacetic acid (DCA) in dichloromethane (DCM) revealed that the loading was 31 μmol/g. The cytidine-loaded CPG was dried under vacuum and stored in a desiccator at room temperature.

3.5.2. Coupling. Trityl-protected, cytidine-loaded CPG (60 mg) was placed in a screw cap vial with a coarse fritted bottom and stopcock and the trityl protecting group was removed, exposing the 5′-amine, with the addition of 10 mL 2% DCA in DCM. The CPG was washed 8 mL of DCM, followed by 10 mL DMF, then soaked in DMF (2 mL for 2 h prior to initial coupling. The 25 mg (20 equiv) of N^4-benzoyl-3′-NH-Fmoc-5′-NH-MMTr-2′,3′,5′-deoxycytidine monomer **13** was dissolved in 1 mL DMF and 5 mg $HgCl_2$ (2 equiv) and 7 μL TEA were separately dissolved in 0.5 mL DMF each. The DMF was removed from the pre-soaked cytidine-loaded CPG and the 1 mL coupling monomer in DMF solution was added, followed by the simultaneous addition of the $HgCl_2$ and TEA in DMF solutions. A fine yellow-white precipitate immediately formed and the vial was fitted with a Teflon gasket and capped tightly, then agitated gently for 1.5 h at room temperature.

3.5.3. Capping. After removing the coupling solution and washing with DMF, the CPG retained a slight gray color due to remaining mercury(I) sulfide precipitate. This was removed by washing with 10 mL of 20% thiolphenol in DMF, followed by copious amounts of DMF. Any unreacted amines were capped by the addition of 1 mL of

100 mM acetic anhydride in DMF and 1 mL of 200 mM TEA in DMF. The reaction mixture was sealed and agitated for 10 min at room temperature then filtered off and washed with 10 mL of DMF, 10 mL MeOH, and finally an additional 10 mL of DMF.

3.5.4. Trityl-deprotection and assay. To prepare for the next coupling and to assay the yield of the last coupling, the 5′-trityl moiety was removed with 10 mL 2% DCA in DCM. The bright yellow deprotection solution was collected and a 20 μL aliquot was diluted into 980 μL of 60% perchloric acid in absolute ethanol. This sample was UV-analyzed to determine the total monomethoxy-trityl cation released, and thus the molarity of monomer coupled.

3.5.5. Cycle repeated. The coupling/capping/deblocking cycle was repeated six times, yielding a heptamer. After the seventh coupling reaction, the capping and deblocking steps were skipped to allow the monomethoxytrityl protecting group to remain on the final octamer, facilitating HPLC purification. The coupling yields were estimated by trityl-UV analysis to be as follows: first coupling (dimer) was 99%; second coupling (trimer) was 98%; third coupling was 96%; fourth coupling was 92%; fifth coupling was 91%, sixth 86%. Because the trityl protecting group was not removed after the seventh coupling, no estimation could be made.

3.5.6. Cleavage and base-labile deprotection. After the seventh coupling, the solid support was washed with the thiophenol/DMF solution followed by copious amounts of DMF and finally MeOH. The reaction vial was dried under vacuum overnight to remove all traces of solvent. The CPG was transferred to a pressure resistant vial, a 4 mL solution of methanolic ammonia was added, and the vial was sealed and placed in a 60 °C oven for 20 h to cleave the oligomer from the solid support and remove base-labile protecting groups. After cooling, the deprotection solution was removed by vacuum centrifugation, yielding a white residue containing the crude trityl-protected octameric cytidine.

3.5.7. HPLC purification. A gradient from 100% eluent A (100 mM triethylammonium acetate, pH 7.0) to 90% eluent B (acetonitrile) over 40 min with a flow rate of 1.5 mL/min was used. Fractions containing the purified oligomer were collected and lyophilized in a Labconco® CentriVap® concentrator. The DNG-C_8 oligomer was characterized by ESI high-resolution mass spectrometry; $(M+H)^+$ 2256.1062, found 2256.1034. After 2% TFA in DCM treatment, to remove the 5′-trityl protecting group, the HPLC purification was repeated. The fully deprotected oligomer was characterized by ESI high-resolution mass spectrometry; $(M+H)^+$ 1983.9861, found 1983.9888.

3.6. Synthesis of cytidine monomers

The monomers used in the solid-phase synthesis (Schemes 1 and 2) were prepared according to Scheme 4. Recent work in synthesizing ribonucleic guanidine (RNG) elucidated a quick path to the final coupling monomer beginning with a 3′,5′-diamino ribonucleoside and this route has now been applied to the deoxynucleic monomers as well.

3.7. N^4-Benzoyl-2′-deoxycytidine (1)[26]

2′-Deoxycytidine (3.31 g; 14.6 mmol) was suspended in anhydrous pyridine and cooled to 0 °C in an ice bath while stirring under argon. Chlorotrimethylsilane (9.24 mL; 5 equiv) was added dropwise with a syringe and the mixture was stirred for 30 min. Benzoyl chloride (8.45 mL; 5 equiv) was added dropwise with a syringe and the mixture was removed from the ice bath and allowed to stir at room temperature for 2 h. After again cooling to 0 °C while stirring, ice cold distilled water (20 mL) was slowly added and followed by the slow addition of concentrated aqueous ammonia (20 mL), 15 min later. After 30 min the reaction mixture was rotovapped to a minimum volume and distilled water (100 mL) added, then filtered through filter paper. The aqueous filtrate was extracted with diethyl ether (2×100 mL), causing crystals to immediately form, and was placed in the refrigerator overnight. Crystals were filtered off and vacuum dried yielding 4.155 g (86%) of pure material. TLC (1:5, MeOH–EtOAc) $R_f = 0.20$; LRMS (ESI) m/z calculated for $C_{16}H_{17}N_3O_5$ $(M+H)^+$ 332.1168, found 332.1120; ^{1}H NMR (400 MHz DMSO-d_6) δ (ppm) 2.00 (d, 1H, 3′-OH), 2.15 (dd, 1H, 5′-OH), 2.28 (m, 2H, 2′-H_2), 3.68 (m, 1H, 3′-H), 3.76 (m, 2H, 5′-H_2), 3.95 (m, 1H, 4′-H), 4.66 (dd, 1H, H^5), 4.74 (dd, 1H, 1′-H), 7.32 (d, 1H, H^6), 7.40–7.85 (m, 5H, N^4-Bz), 8.25 (s, 1H, N^4-H).

3.8. N^4-Benzoyl-3′,5′-*O*-dimesyl-2′-deoxycytidine (2)

N^4-Benzoyl-2′-deoxycytidne **1** (3.72 g; 11.2 mmol) was dissolved in anhydrous pyridine (60 mL) and stirred under argon at 0 °C while methanesulfonyl chloride (1.74 mL; 2 equiv) was added dropwise with a syringe. The reaction mixture was allowed to come to room temperature over 2 h and the product was then precipitated by pouring into vigorously stirring ice water (350 mL) and maximized by refrigerating overnight. The solid was filtered, washed with cold water, and dried under vacuum to give 5.32 g of white powder (97%). TLC (1:5, MeOH–methylene chloride) $R_f = 0.55$; LRMS (ESI) m/z calculated for $C_{17}H_{19}N_3O_7S$ $(M+H)^+$ 488.0719, found 488.0705. ^{1}H NMR (400 MHz DMSO-d_6) δ (ppm) 2.27 (m, 2H, 2′-H_2), 3.14 (s, 3H, Ms-CH_3), 3.18 (s, 3H, Ms-CH_3), 3.69 (m, 1H, 3′-H), 3.77 (m, 2H, 5′-H_2), 3.95 (m, 1H, 4′-H), 4.67 (dd, 1H, H^5), 4.73 (dd, 1H, 1′-H), 7.31 (d, 1H, H^6), 7.39–7.85 (m, 5H, N^4-Bz), 8.24 (s, 1H, N^4-H).

3.9. N^4-Benzoyl-5′-*O*-mesyl-2,3′-anhydro-2′-deoxycytidine (3)

N^4-Benzoyl-3′,5′-*O*-dimesyl-2′-deoxycytidine **2** (5.32 g; 10.9 mmol) was dissolved in anhydrous *N*,*N*-dimethylformamide (80 mL), potassium phthalimide (4.0 g;

2 equiv) was added, and the mixture was heated to 90 °C for 15 min while stirring under argon then allowed to cool to room temperature. The solid was removed by filtration, washed with 40 mL of DMF and the filtrates were concentrated under vacuum to a yellow solid, and dried under vacuum overnight. The crude product was dissolved acetone/MeOH (2:1) and adsorbed on silica gel then loaded onto a pre-existing silica column and eluted with acetone. Pure fractions collected were concentrated under vacuum to yield 3.0 g (60%) of white foam. TLC (acetone) $R_f = 0.50$; LRMS (ESI) m/z calculated for $C_{16}H_{16}N_6O_4$ $(M+H)^+$ 392.0838, found 392.0850. ^{1}H NMR (400 MHz DMSO-d_6) δ (ppm) 2.25 (m, 2H, 2′-H_2), 3.05 (s, 3H, Ms-CH_3), 3.52 (m, 1H, 3′-H), 3.62 (m, 2H, 5′-H_2), 3.94 (m, 1H, 4′-H), 4.79 (dd, 1H, 1′-H), 5.67 (dd, 1H, H^5), 7.21 (d, 1H, H^6), 7.38–7.84 (m, 5H, N^4-Bz).

3.10. 3′,5′-Diazido-N^4-benzoyl-2′,3′,5′-deoxycytidine (4)

N^4-Benzoyl-5′-*O*-mesyl-2,3′-anhydro-2′-deoxycytidine **3** (1.79 g; 4.58 mmol) and LiN_3 (4.48 g; 2 equiv) were dissolved in anhydrous DMF (40 mL) at 90 °C while stirring under argon for 4 h, then concentrated to a solid under vacuum. CH_3Cl (50 mL) was added and the mixture was sonicated, filtered, and the filtrate reduced to a minimum volume. The filtrate was eluted through a silica column with CH_3Cl and pure fractions were concentrated under vacuum to yield 0.680 g (70%) of white foam. TLC (1:5, MeOH–methylene chloride) $R_f = 0.60$; LRMS (ESI) m/z calculated for $C_{22}H_{28}N_4O_5$ $(M+H)^+$ 382.1298, found 382.1278. ^{1}H NMR (400 MHz DMSO-d_6) δ (ppm) 1.68 (m, 2H, 5′-H_2), 1.98 (m, 1H, 3′-H), 2.19 (m, 2H, 2′-H_2), 3.92 (m, 1H, 4′-H), 4.57 (dd, 1H, H^5), 5.79 (dd, 1H, 1′-H), 7.20 (d, 1H, H^6), 7.37–7.83 (m, 5H, N^4-Bz), 8.05 (s, 1H, N^4-H).

3.11. 3′,5′-Diamino-N^4-benzoyl-2′,3′,5′-deoxycytidine (5)

3′,5′-Diazido-N^4-benzoyl-2′,3′,5′-deoxycytidine **4** (0.600 g; 1.57 mmol) was dissolved in anhydrous ethanol, a catalytic amount of activated palladium on carbon was added, and the mixture hydrogenated (50 psi) for 4 h then filtered through Celite, and concentrated under vacuum to yield 0.517 g (100%) of white foam. TLC (1:1, MeOH–EtOAc) $R_f = 0.25$; LRMS (ESI) m/z calculated for $C_{23}H_{30}N_4O_7S$ $(M+H)^+$ 330.1488, found 330.1479. ^{1}H NMR (400 MHz DMSO-d_6) δ (ppm) 2.01 (dd, 2H, 3′-NH_2), 2.26 (m, 2H, 5′-NH_2), 2.41 (m, 2H, 2′-H_2), 2.68 (m, 2H, 5′-H_2), 2.98 (m, 1H, 3′-H), 4.22 (m, 1H, 4′-H), 4.57 (dd, 1H, H^5), 5.82 (dd, 1H, 1′-H), 7.22 (d, 1H, H^6), 7.42–7.92 (m, 5H, N^4-Bz), 8.17 (s, 1H, N^4-H).

3.12. 3′-Amino-N^4-benzoyl-5′-NH-MMTr-2′,3′,5′-deoxycytidine (6)

3′,5′-Diamino-N^4-benzoyl-2′,3′,5′-deoxycytidine **5** (0.350 g; 1.06 mmol) and MMTrCl (0.029 g; 0.9 equiv) were cooled to −70 °C under argon then suspended in anhydrous TEA (10 mL) with stirring and allowed to come to room temperature overnight. The reaction mixture was cooled again to −70 °C and anhydrous CH_2Cl_2 (20 mL) was added drop wise and the mixture was allowed to warm to room temperature. H_2O (20 mL) was added and the mixture was vigorously shaken, then centrifuged. The top organic layer was removed and concentrated to a solid under vacuum, then re-dissolved in 5% MeOH/1% TEA in CH_2Cl_2 and eluted with the same mixture on a silica column to afford the pure product as 0.320 g (50%) of white solid. TLC (EtOAc) $R_f = 0.45$; LRMS (ESI) m/z calculated for $C_{21}H_{26}N_4O_5$ $(M+H)^+$ 602.2689, found 602.2696. ^{1}H NMR (400 MHz DMSO-d_6) δ (ppm) 1.94 (m, 2H, 5′-NH), 2.15 (dd, 2H, 3′-NH_2), 2.34 (m, 2H, 2′-H_2), 2.67 (m, 2H, 5′-H_2), 2.97 (m, 1H, 3′-H), 3.75 (s, 3H, MMTr-*p*-OMe), 4.22 (m, 1H, 4′-H), 4.57 (dd, 1H, H^5), 5.82 (dd, 1H, 1′-H), 6.63–7.17 (m, 15H, MMTr-H), 7.24 (d, 1H, H^6), 7.42–7.92 (m, 5H, N^4-Bz), 8.16 (s, 1H, N^4-H).

3.13. N^4-Benzoyl-3′-NH-FmocNCS-5′-NH-MMTr-2′,3′,5′-deoxycytidine (7)

3′-Amino-N^4-benzoyl-5′-NH-MMTr-2′,3′,5′-deoxycytidine **6** (0.320 g; 0.53 mmol) was dissolved in DCM (20 mL), Fmoc-NCS (0.031 g; 1.5 equiv) was added as a solid, and the mixture was allowed to stir under argon at room temperature for 1 h. H_2O (20 mL) was added; the mixture was shaken vigorously and then centrifuged. The top organic layer was removed and concentrated to a solid under vacuum, then re-dissolved in EtOAc and eluted with the same mixture on a silica column, which had previously been eluted with 5% TEA in EtOAc, then washed with only EtOAc, to afford the pure product as 0.140 g (30%) of white solid. TLC (1:1, hexanes–EtOAc) $R_f = 0.60$; LRMS (ESI) m/z calculated for $C_{52}H_{46}N_6O_6S$ $(M+H)^+$ 883.3200, found 883.3243. ^{1}H NMR (400 MHz DMSO-d_6) δ (ppm) 2.01 (m, 2H, 5′-NH), 2.16 (dd, 1H, 3′-NH), 2.30 (m, 2H, 2′-H_2), 2.67 (m, 2H, 5′-H_2), 2.97 (m, 1H, 3′-H), 3.74 (s, 3H, MMTr-*p*-OMe), 4.33 (m, 2H, Fmoc-CH_2), 4.20 (m, 1H, 4′-H), 4.54 (dd, 1H, H^5), 4.72 (m, 2H, Fmoc-CH_2), 5.82 (dd, 1H, 1′-H), 6.63–7.17 (m, 15H, MMTr-H), 7.24 (d, 1H, H^6), 7.20–7.92 (m, 13H, N^4-Bz + Fmoc-CH), 8.13 (s, 1H, N^4-H), 8.22 (d, 1H, Fmoc-α-H).

Acknowledgements

This work was supported by the National Institutes of Health Grant 5R37DK09171-39. We thank Dr. Renee Szabo for conversations and advice.

References and notes

1. Agrawal, S.; Zhao, Q. Y. Antisense therapeutics. *Curr. Opin. Chem. Biol.* **1998**, *2*(4), 519–528.
2. Demesmaeker, A.; Haner, R.; Martin, P.; Moser, H. E. Antisense Oligonucleotides. *Acc. Chem. Res.* **1995**, *28*(9), 366–374.
3. Zamaratski, E.; Pradeepkumar, P. I.; Chattopadhyaya, J. A critical survey of the structure-function of the antisense

oligo/RNA heteroduplex as substrate for RNase H. *J. Biochem. Biophys. Meth.* **2001**, *48*(3), 189–208.
4. Demesmaeker, A.; Altmann, K. H.; Waldner, A.; Wendeborn, S. Backbone modifications in oligonucleotides and peptide nucleic-acid systems. *Curr. Opin. Struct. Biol.* **1995**, *5*(3), 343–355.
5. Nielsen, P. E. Structural and biological properties of peptide nucleic acid (PNA). *Pure Appl. Chem.* **1998**, *70*(1), 105–110.
6. Peyman, A.; Uhlmann, E.; Wagner, K.; Augustin, S.; Breipohl, G.; Will, D. W.; Schafer, A.; Wallmeier, H. Phosphonic ester nucleic acids (PHONAs): oligonucleotide analogues with an achiral phosphonic acid ester backbone. *Angew. Chem., Int. Ed. Engl.* **1996**, *35*(22), 2636–2638.
7. Fujii, M.; Yoshida, K.; Hidaka, J.; Ohtsu, T. Nucleic acid analog peptide (NAAP). 2. Syntheses and properties of novel DNA analog peptides containing nucleobase linked beta-aminoalanine. *Bioorg. Med. Chem. Lett.* **1997**, *7*(5), 637–640.
8. Summerton, J.; Weller, D. Antisense properties of morpholino oligomers. *Nucleosides Nucleotides* **1997**, *16*(7–9), 889–898.
9. Morvan, F.; Sanghvi, Y. S.; Perbost, M.; Vasseur, J. J.; Bellon, L. Oligonucleotide mimics for antisense therapeutics: Solution phase and automated solid-support synthesis of MMI linked oligomers. *J. Am. Chem. Soc.* **1996**, *118*(1), 255–256.
10. Waldner, A.; Demesmaeker, A.; Lebreton, J.; Fritsch, V.; Wolf, R. M. Ureas as backbone replacements for the phosphodiester linkage in oligonucleotides. *Synlett* **1994**, (1), 57–61.
11. Wang, J. Y.; Matteucci, M. D. The synthesis and binding properties of oligonucleotide analogs containing diastereomerically pure conformationally restricted acetal linkages. *Bioorg. Med. Chem. Lett.* **1997**, *7*(2), 229–232.
12. vonMatt, P.; Altmann, K. H. Replacement of the phosphodiester linkage in oligonucleotides by heterocycles: The effect of triazole- and imidazole-modified backbones on DNA/RNA duplex stability. *Bioorg. Med. Chem. Lett.* **1997**, *7*(12), 1553–1556.
13. Kurreck, J.; Wyszko, E.; Gillen, C.; Erdmann, V. A. Design of antisense oligonucleotides stabilized by locked nucleic acids. *Nucl. Acids Res.* **2002**, *30*(9), 1911–1918.
14. Ueno, Y.; Mikawa, M.; Matsuda, A. Nucleosides and nucleotides. 170. Synthesis and properties of oligodeoxynucleotides containing 5-*N*-2-*N*,*N*-bis(2-aminoethyl)amino ethyl carbamoyl-2′-deoxyuridine and 5-*N*-3-*N*,*N*-bis(3-aminopropyl)amino propyl carbamoyl-2′-deoxyuridine. *Bioconjug. Chem.* **1998**, *9*(1), 33–39.
15. Manoharan, Muthiah; Guinosso, C. J.; Dan Cook, P. Novel functionalization of the sugar moiety of nucleic acids for multiple labeling in the minor groove. *Tetrahedron Lett.* **1991**, *32*(49), 7171–7174.
16. Skibo, E. B.; Xing, C. G. Chemistry and DNA alkylation reactions of aziridinyl quinones: Development of an efficient alkylating agent of the phosphate backbone. *Biochemistry* **1998**, *37*(43), 15199–15213.
17. Jung, P. M.; Histand, G.; Letsinger, R. L. Hybridization of alternating cationic/anionic oligonucleotides to RNA segments. *Nucleosides Nucleotides* **1994**, *13*(6–7), 1597–1605.
18. Chaturvedi, S.; Horn, T.; Letsinger, R. L. Stabilization of triple-stranded oligonucleotide complexes: use of probes containing alternating phosphodiester and stereo-uniform cationic phosphoramidate linkages. *Nucl. Acids Res.* **1996**, *24*(12), 2318–2323.
19. Dempcy, R. O.; Almarsson, O.; Bruice, T. C. Design and synthesis of deoxynucleic guanidine—a polycation analog of DNA. *Proc. Natl. Acad. Sci. U.S.A.* **1994**, *91*(17), 7864–7868.
20. Barawkar, D. A.; Bruice, T. C. Synthesis, biophysical properties, and nuclease resistance properties of mired backbone oligodeoxynucleotides containing cationic internucleoside guanidinium linkages: deoxynucleic guanidine/DNA chimeras. *Proc. Natl. Acad. Sci. U.S.A.* **1998**, *95*(19), 11047–11052.
21. Linkletter, B. A.; Szabo, I. E.; Bruice, T. C. Solid-phase synthesis of deoxynucleic guanidine (DNG) oligomers and melting point and circular dichroism analysis of binding fidelity of octameric thymidyl oligomers with DNA oligomers. *J. Am. Chem. Soc.* **1999**, *121*(16), 3888–3896.
22. Linkletter, B. A.; Szabo, I. E.; Bruice, T. C. Solid-phase synthesis of oligopurine deoxynucleic guanidine (DNG) and analysis of binding with DNA oligomers. *Nucl. Acids Res.* **2001**, *29*(11), 2370–2376.
23. Kojima, N.; Bruice, T. C. Replacement of the phosphorodiester linkages of RNA with guanidinium linkages: the solid-phase synthesis of ribonucleic guanidine. *Org. Lett.* **2000**, *2*(1), 81–84.
24. Kojima, N.; Szabo, I. E.; Bruice, T. C. Synthesis of ribonucleic guanidine: replacement of the negative phosphodiester linkages of RNA with positive guanidinium linkages. *Tetrahedron* **2002**, *58*(5), 867–879.
25. Dempcy, R. O.; Browne, K. A.; Bruice, T. C. Synthesis of the polycation thymidyl DNG, its fidelity in binding polyanionic DNA/RNA, and the stability and nature of the hybrid complexes. *J. Am. Chem. Soc.* **1995**, *117*(22), 6140–6141.
26. Gait, M. J. In *Oligonucleotide Synthesis: A Practical Approach*; IRL: Oxford Oxfordshire; Washington, DC, 1984; Vol. p 13, p 217.
27. Horwitz, J. P.; Chua, J.; Noel, M.; Donatti, J. T. Nucleosides. 11. 2′,3′-dideoxycytidin. *J. Org. Chem.* **1967**, *32*(3), 817.
28. Kearney, P. C.; Fernandez, M.; Flygare, J. A. Solid-phase synthesis of 2-aminothiazoles. *J. Org. Chem.* **1998**, *63*(1), 196–200.
29. Simonsson, T. G-quadruplex DNA structures—variations on a theme. *Biolog. Chem.* **2001**, *382*(4), 621–628.
30. Gilbert, D. E.; Feigon, J. Multistranded DNA structures. *Curr. Opin. Struct. Biol.* **1999**, *9*(3), 305–314.
31. Zarudnaya, M. I.; Samijlenko, S. P.; Potyahaylo, A. L.; Hovorun, D. M. Structural transitions in polycytidylic acid: proton buffer capacity data. *Nucleosides Nucleotides Nucl. Acids* **2002**, *21*(2), 125–137.
32. Gueron, M.; Leroy, J.-L. The *i*-motif in nucleic acids. *Curr. Opin. Struct. Biol.* **2000**, *10*(3), 326–331.
33. Saenger, W.. In: *Principles of Nucleic Acid Structure*; Springer: New York, 1984; Vol. p 20, p 556.
34. Mergny, J.; Lacroix, L. Kinetics and thermodynamics of i-DNA formation: phosphodiester versus modified oligodeoxynucleotides. *Nucl. Acids Res.* **1998**, *26*(21), 4797–4803.
35. Job, P. Formation and stability of inorganic complexes in solution. *Ann. Chim.* **1928**, *9*, 113–203.
36. Tinoco, I. Nucleic acid structures, energetics, and dynamics. *J. Phys. Chem.* **1996**, *100*(31), 13311–13322.
37. Luo, J.; Bruice, T. C. Nanosecond molecular dynamics of hybrid triplex and duplex of polycation deoxyribonucleic guanidine strands with a complimentary DNA strand. *J. Am. Chem. Soc.* **1998**, *120*(6), 1115–1123.
38. MathWorks *Matlab*, MATLAB Version 6.5 Release 13; The MathWorks, Inc.: 2002.
39. Henry, E. R.; Hofrichter, J. Singular value decomposition—application to analysis of experimental-data. *Meth. Enzymol.* **1992**, *210*, 129–192.
40. Hendler, R. W.; Shrager, R. I. Deconvolutions based on singular-value decomposition and the pseudoinverse—a

guide for beginners. *J. Biochem. Biophys. Meth.* **1994**, *28*(1), 1–33.
41. Haq, I.; Chowdhury, B. Z.; Chaires, J. B. Singular value decomposition of 3-D DNA melting curves reveals complexity in the melting process. *Eur. Biophys. J. Biophys. Lett.* **1997**, *26*(6), 419–426.
42. Murchie, A. I. H.; Aboul-ela, F.; Laughlan, G.; Luisi, B.; Lilley, D. M. J. Structure of parallel-stranded guanine tetraplexes. *Nucl. Acids Mol. Biol.* **1995**, *9*, 143–164.
43. Pinnavaia, T. J.; Marshall, C. L.; Mettler, C. M.; Fisk, C. I.; Miles, H. T.; Becker, E. D. Alkali-metal ion specificity in solution ordering of a nucleotide, 5′-guanosine monophosphate. *J. Am. Chem. Soc.* **1978**, *100*(11), 3625–3627.
44. Marky, L. A.; Breslauer, K. J. Calculating thermodynamic data for transitions of any molecularity from equilibrium melting curves. *Biopolymers* **1987**, *26*, 1601–1620.